FRP CONFINED CONCRETE STRESS-STRAIN MODEL UTILIZING A VARIABLE STRAIN DUCTILITY RATIO

By Domingo A. Moran[1] and Chris P. Pantelides[2]

A model for representing the compressive behavior of concrete members confined using FRP composite jackets is presented. The distinguishing feature of the analytical model is that the plastic behavior of the FRP-confined concrete can be represented by an experimentally derived variable strain ductility ratio, which defines the increase in plastic axial compressive strain versus the increase in plastic axial compressive strength of the FRP-confined concrete. This is demonstrated to be a function of the stiffness of the confining FRP jacket and the extent of internal damage, rather than a constant as is typically assumed for steel confined concrete. The model predicts that the plastic dilation rate of FRP-confined concrete is a function of the confining stiffness of the FRP jacket and the type of FRP jacket construction, be it bonded or non-bonded. An expression was obtained for predicting the ultimate compressive strength and strain of FRP- confined concrete based on equilibrium and plasticity analysis. The ultimate compressive strength and strain of the FRP-confined concrete were found to be a function of the jacket stiffness, the type of jacket construction, and the ultimate strain in the FRP jacket. Comparisons with experimental results indicate good agreement.

INTRODUCTION

The retrofit of reinforced concrete columns with FRP composite jackets has become increasingly common in regions of high seismicity. A significant amount of research has been carried out on the use of FRP composite jackets for the seismic retrofit and repair of existing reinforced concrete columns and bridge systems (Saadatmanesh et al. 1994, Seible et al. 1997, Xiao and Ma 1997, Pantelides et al. 1999).

The compressive stress-strain behavior of FRP confined concrete cylinders is essentially nonlinear. The initial portion of the stress-strain response typically follows that of the unconfined concrete. After achieving the unconfined concrete strength, the response of the FRP-confined concrete softens, this softening can occur with either a localized descending branch that may stabilize as the dilation of the concrete core progresses, or it may exhibit a <u>bilinear</u> behavior until the FRP composite jacket fails.

Several investigators have introduced stress-strain models for concrete confined by FRP jackets. Two very promising models are those introduced by Xiao and Wu (2000) and Spoelstra and Monti (1999). The Xiao and Wu (2000) model is an elasticity based bilinear model in which the behavior of the FRP confined concrete is described in terms of the mechanical properties of the concrete core and the confining FRP jacket. The Spoelstra and Monti (1999) model, is an iterative equilibrium-based model in which the behavior of the FRP confined concrete is governed by both the Mander et al. (1988) model for steel confined concrete and the Pantazopoulou and Mills (1995) constitutive model for concrete.

[1] Engineer, Reaveley Engineers and Assoc., Salt Lake City, UT 84106
[2] Prof., Dept. of Civil and Envr. Eng., Univ. of Utah, Salt Lake City, UT 84112.

In the Mander et al. (1988) model for steel confined concrete, the increase in the peak compressive strength of the confined concrete is expressed in terms of a constant effective confining pressure, and a resultant constant strain ductility ratio that defines the increase in the compressive strain relative to the increase in the compressive strength of the steel confined concrete. By contrast, the model proposed herein is based on an internal damage failure surface that determines the increase in the plastic compressive strength of the FRP-confined concrete. A variable strain ductility ratio is introduced, in which the increase in the plastic compressive strain of the FRP-confined concrete is shown to be a function of the hoop stiffness of the FRP composite jacket and the extent of internal damage in the concrete core.

CONFINEMENT EFFECTIVENESS OF FRP-CONFINED CONCRETE

The confinement effectiveness, k_{cc}, of the confining element, is typically defined by the well known Richart et al. (1928) relationship in which:

$$k_{cc} = \frac{f_{cc}}{f_{co}} = 1 + k_1 k_r\ ;\ \ k_r = \frac{f_r}{f_{co}} \tag{1}$$

where $k_1 =$ confinement coefficient, $k_r =$ confinement ratio and $f_r =$ average confining pressure. In Fig. 1, a typical stress-strain curve is shown in terms of the normalized compressive stress $\left(k_c\right)_i$ versus the effective confinement ratio $\left(k_{re}\right)_i$ of members exhibiting strain hardening plastic behavior. By examining the stress-strain behavior of concrete cylinder tests of specimens confined by non-bonded Glass FRP composite jackets (GFRP), performed by Mirmiran (1997), and cylinders confined by bonded Carbon FRP composite jackets (CFRP), performed by Xiao and Wu (2000), it was found that on average the plastic region of the compressive stress-strain behavior tends to initiate at an average plastic strain $\left(\varepsilon_{\theta p}\right)_o$, see Fig. 1, where for non-bonded FRP jacketed cylinders $\left(\varepsilon_{\theta p}\right)_o \approx 5.0$ mm/m, and for bonded FRP jacketed cylinders $\left(\varepsilon_{\theta p}\right)_o \approx 3.0$ mm/m. Also, by selecting a series of plastic jacket strains, $\left(\varepsilon_{\theta p}\right)_i$, that are within the range $\left(\varepsilon_{\theta p}\right)_o \le \left(\varepsilon_{\theta p}\right)_i \le \left(\varepsilon_{\theta}\right)_u$ where $\varepsilon_{\theta u} =$ ultimate radial jacket strain, as shown in Fig. 1. The following is proposed for circular concrete members, confined by circular strap or continuous FRP jackets, in which the plastic confinement effectiveness $\left(k_{cp}\right)_i$ of FRP confined concrete is defined as:

$$\left(k_{cp}\right)_i = \frac{\left(f_{cp}\right)_i}{f_{co}} = 1 + \left(k_{1p}\right)_i \left(k_{re}\right)_i \tag{2}$$

$$\left(k_{1p}\right)_i = \left(\alpha_p\right)_i \left(k_1\right)_{avg};\ \ \left(\alpha_p\right)_i = \left(1 - \frac{\gamma_p}{\left(k_{re}\right)_i^2}\right) \tag{3}$$

$$\left(k_{re}\right)_i = \frac{\left(f_{re}\right)_i}{f_{co}} = \frac{C_j \left(\varepsilon_\theta\right)_i k_{\mathrm{e}}}{f_{co}} = K_{je}\left(\varepsilon_\theta\right)_i;\ K_{je} = K_j k_e \tag{4}$$

$$K_j = \frac{C_j}{f_{co}};\quad C_j = \frac{2 t_j E_j}{D_c} \tag{5}$$

where t_j = jacket thickness, E_j = jacket tangent hoop modulus of elasticity, D_c = concrete column diameter, f_{co} = unconfined concrete core compressive strength, C_j = hoop jacket stiffness, K_j = normalized jacket stiffness, $(f_{re})_i$ = effective confining pressure, k_e = confinement efficiency of the FRP jacket that accounts for arching of passive confining stresses, where $0 \le k_e \le 1.0$; for circular continuous FRP jackets $k_e = 1.0$. Also $(k_{re})_i$ = effective confinement ratio and $(f_{cp})_i$ = plastic compressive stress at a given plastic radial strain, $(\varepsilon_{\theta p})_i$, in the confining FRP jacket. In (3) the term $(\alpha_p)_i$ = variable confinement coefficient. Regression analysis suggests that for non-bonded FRP confined concrete $\gamma_p = 9.1x10^{-3}$ and $\gamma_p = 1.7x10^{-3}$ for bonded. In Figs. 2(a) and 2(b) the experimental $(k_{1p})_i$ determined using (2) is plotted versus the effective confinement ratio, $(k_{re})_i$, of (4), for both non-bonded and bonded FRP confined concrete, respectively. In these figures, it can be observed that at high effective confinement ratios, $(k_{re})_i$, the experimental $(k_{1p})_i$ approaches an average asymptotic value of $(k_1)_{avg} \approx 2.3$ for non-bonded and $(k_1)_{avg} \approx 4.1$ for bonded FRP confined concrete. Also, in these figures the analytical $(k_{1p})_i$ of (3) is plotted as solid lines. Using (2)-(5) the following analytical relationship $(k_{cp})_i$, can be obtained as follows:

$$(k_{cp})_i = \frac{(f_{cp})_i}{f_{co}} = 1 + \omega_{je}(\alpha_p)_i(\varepsilon_{\theta p})_i \; ; \; \omega_{je} = K_{je}(k_1)_{avg} \tag{6}$$

where ω_{je} = bond-dependent effective confinement index. In Figures 3(a) and 3(b) the experimental $(k_{cp})_i$, is plotted versus $(k_{re})_i$ for non-bonded and bonded FRP confined concrete, respectively. In these figures, the above relationship for the analytical $(k_{cp})_i$ is plotted as a solid line. In this article, only those FRP-confined concrete members that exhibit a strain hardening plastic behavior (i.e. a positive plastic slope) are considered; these may include both circular sections and rectangular sections having appropriate corner radii and sufficient effective jacket stiffness. This occurs when $(\alpha_p)_i \ge 0$, which from (3) occurs at a critical confinement ratio, $(k_{re})_{cr} = \sqrt{\gamma_p}$; this is the confinement ratio below which (3) predicts that $(k_{1p})_i \le 0$, and below which (2) and (6) predict that $(k_{cp})_i \le 1.0$.

VARIABLE STRAIN DUCTILITY RATIO OF FRP-CONFINED CONCRETE

The increase in strain ductility of concrete confined by either steel reinforcement, steel jackets, or FRP composite jackets can be found from the definition of the strain ductility ratio R, as shown in Fig. 4, which was proposed by Mander et al. (1988) as:

$$R = \frac{k_\varepsilon - 1}{k_{cc} - 1} \; ; \; \mathrm{k}_\varepsilon = \frac{\varepsilon_{cc}}{\varepsilon_{co}} \tag{7}$$

where (k_{cc}) is defined in (1), $k_\varepsilon =$ compressive strain effectiveness, $\varepsilon_{co} =$ peak compressive strain of the unconfined concrete core, where typically $\varepsilon_{co} \approx 2.0$ mm/m, and $\varepsilon_{cc} =$ peak compressive strain of the confined concrete, as shown in Fig. 4. For concrete in a biaxial compression state of stress, Darwin and Pecknold (1977) indicate that R is a constant, where $R = 3$; for steel confined concrete Mander et al. (1988) indicate that R is also a constant, where $R = 5.0$. In the case of FRP-confined concrete, the experimental data suggest that the plastic strain ductility ratio $(R_p)_i$, as shown in Fig. 5, varies as the internal damage (i.e. $(\varepsilon_{\theta p})_i$) of the concrete core progresess, where:

$$(R_p)_i = \frac{(\lambda_p)_i}{(k_{cp})_i - 1} \quad ; \quad (\lambda_p)_i = (k_{\varepsilon p})_i - 1 \; ; \quad (k_{\varepsilon p})_i = \frac{(\varepsilon_{cp})_i}{\varepsilon_{co}} \tag{8}$$

and $(k_{cp})_i$ is defined in (2) and (6), $(\varepsilon_{cp})_i =$ plastic compressive strain, and $(\lambda_p)_i =$ axial plastic compressive strain ratio at a given plastic radial strain $(\varepsilon_{\theta p})_i$. From the analysis of the experimental data and the use of (8) and Fig. 6, the following relationship for the analytical compressive strain $\left(\bar{\lambda}_p\right)_i$ and strain ductility $\left(\bar{R}_p\right)_i$ ratios are proposed:

$$\left(\bar{\lambda}_p\right)_i = \frac{1}{\psi_p}(K_{je})\left[\, (\varepsilon_{\theta p})_i - \varepsilon_{\theta o}\right] ; \;\; \varepsilon_{\theta o} = (\varepsilon_{\theta p})_o - |\varepsilon_{co}| \; ; \;\; \psi_p = k_p(\omega_{je})^{\beta_p} \tag{9}$$

$$\left(\bar{R}_p\right)_i = \left[\frac{(\Delta_\varepsilon)_i}{(k_{1p})_i \psi_p}\right] ; \;\; (\Delta_\varepsilon)_i = \left(\frac{(\varepsilon_{\theta p})_i - \varepsilon_{\theta o}}{(\varepsilon_{\theta p})_i}\right) \tag{10}$$

where $\varepsilon_{\theta o} =$ increment in radial strain, as shown in Fig. 6; $\psi_p =$ kinematic restraint coefficient in which, for non-bonded FRP confined concrete the constants are $\beta_p = 0.30$ and $k_p = 7.4x10^{-3}$, and for bonded $\beta_p = 0.45$ and $k_p = 3.4x10^{-3}$. Also $(\Delta_\varepsilon)_i =$ internal damage coefficient that determines the degree of internal damage due to the dilation of the FRP-confined concrete core; when $(\varepsilon_{\theta p})_i$ becomes large $(\Delta_\varepsilon)_i \to 1.0$, failure of the FRP jacket is imminent. In Figs. 7(a) and 7(b), the experimental $(R_p)_i$ and analytical $\left(\bar{R}_p\right)_i$ calculated using (8) and (10) are plotted versus the stress ratio, $\left[\, (k_{cp})_i - 1\right]$, at an experimental plastic radial strain $(\varepsilon_{\theta p})_i =$ 5 mm/m for non-bonded GFRP and bonded CFRP confined concrete, respectively. From these figures it can be observed that (10) can accurately capture the variation of the experimental plastic strain ductility ratio.

In modeling the non-linear compressive behavior of FRP confined concrete, Mirmiran (1997), Mirmiran and Shahawy (1996, 1997a, 1997b), and Samaan, et al. (1998) introduced the concept of an ultimate dilation rate (μ_u), defined as:

$$\mu_u = \left|\frac{d\varepsilon_\theta}{d\varepsilon_c}\right|_u = \frac{E_{cp}}{E_{\theta p}} \tag{11}$$

where $\varepsilon_\theta =$ average radial strain and $\varepsilon_c =$ average axial strain in the concrete member, $E_{cp} =$ axial plastic modulus and $E_{\theta p} =$ radial plastic modulus. Mirmiran and Shahawy (1997a, 1997b), Samaan et al. (1998), Stanton et al. (1999), and Xiao and Wu (2000) have suggested a series of predictive relationships for the ultimate dilation rate, μ_u, in terms of the normalized confining stiffness, K_j, of (5). Using the definition of the dilation rate of (11) and using (6), (8) and (9), and the use of Fig. 8, a bond-dependent asymptotic plastic dilation rate, (μ_p), is introduced herein, where:

$$\mu_p = \left(\frac{d\varepsilon_{\theta p}}{d\varepsilon_{cp}}\right)_i = \frac{\left(E_{cp}\right)_i}{\left(E_{\theta p}\right)_i} = \frac{\left(\varepsilon_{\theta p}\right)_i - \left(\varepsilon_{\theta p}\right)_{i-1}}{\left(\varepsilon_{cp}\right)_i - \left(\varepsilon_{cp}\right)_{i-1}} = \frac{\psi_p}{\varepsilon_{co} K_{je}} \tag{12}$$

The analytical plastic dilation rate, (μ_p), of (12) is plotted as a solid line in Fig. 9(a) and 9(b) versus the effective jacket confining stiffness, (K_{je}), of non-bonded GFRP and bonded CFRP confined concrete cylinder tests, respectively. From these figures, it can be observed that (12) can accurately capture the variation of the platic dilation rate, (μ_p), with respect to the effective stiffness, K_{je}, of the confining FRP jacket. Solving for (ψ_p) in (12), substituting it into (9), and further solving for the axial plastic compressive strain, $\left(\varepsilon_{cp}\right)_i$, in (8) yields:

$$\left(\varepsilon_{cp}\right)_i = \varepsilon_{co}\left[1 + \frac{\left(\Delta_\theta\right)_i}{\mu_p}\right] ; \quad \left(\Delta_\theta\right)_i = \frac{\left(\varepsilon_{\theta p}\right)_i - \varepsilon_{\theta o}}{\varepsilon_{co}} \tag{13}$$

where $\left(\Delta_\theta\right)_i =$ radial strain ratio. Thus, at a given plastic radial strain $\left(\varepsilon_{\theta p}\right)_i$, in which $\left(\varepsilon_{\theta p}\right)_o \le \left(\varepsilon_{\theta p}\right)_i \le \left(\varepsilon_\theta\right)_u$, a stress-strain coordinate, $\left(f_{cp}, \varepsilon_{cp}\right)_i$, in the plastic region of the compressive behavior of the FRP-confined concrete can now be predicted. At a given plastic radial strain, $\left(\varepsilon_{\theta p}\right)_i$, (6) and (13) can be used to predict the plastic compressive stress, $\left(f_{cp}\right)_i$, and the axial plastic compressive strain, $\left(\varepsilon_{cp}\right)_i$, respectively.

STRESS-STRAIN MODEL

The stress-strain model developed herein is based on a typical compressive stress-strain behavior of an FRP-confined concrete member that exhibits a bilinear compressive behavior, as shown in both

Figs. 8 and 10, is assumed herein to describe the behavior of FRP-confined concrete, where for convenience only the absolute values of strain and stress are considered:

$$f_c = (E_s)_m \varepsilon_m ; \; (E_s)_m = \left[\frac{(E_m - E_{mp})}{\left(1 + \left| \frac{(E_m - E_{mp})\varepsilon_m}{f_{om}} \right|^{n_m} \right)^{\frac{1}{n_m}}} + E_{mp} \right] \tag{14}$$

$$E_{cp} = \left(\frac{E_{\theta p}}{\mu_p} \right); \; E_{\theta p} = f_{co}\omega_{je}\varphi_\theta ; \; \varphi_\theta = \frac{1}{1-\eta}\left[(\alpha_p)_i - \eta (\alpha_p)_{i-1} \right] \tag{15}$$

$$E_c \approx 4733\sqrt{f_{co}} \; MPa \; \left(57{,}000\sqrt{f_{co}} \; psi \right); \; E_\theta = \frac{E_c}{\mu_o} \tag{16}$$

$$(k_o)_\theta = \frac{(f_o)_\theta}{f_{co}} = 1 + \omega_{je}(\varepsilon_{\theta p})_i \left[\, (\alpha_p)_i - \varphi_\theta \right] \tag{17}$$

$$(k_o)_c = \frac{(f_o)_c}{f_{co}} = (k_o)_\theta + \left(\frac{E_{\theta p}}{f_{co}} \right) \left\{ \, (\varepsilon_{\theta p})_i - \varepsilon_{co}\left[\mu_p + (\Delta_\theta)_i \right] \right\} \tag{18}$$

where: $(E_s)_m$ = variable secant modulus evaluated at the strain ε_m, which is governed by the Richard and Abbott (1975) model. In addition, E_{mp} = average plastic modulus in either the axial (E_{cp}) or radial $(E_{\theta p})$ strain direction, E_m = tangent modulus of elasticity in either the axial (E_c) or radial (E_θ) strain direction, μ_o = initial Poisson's ratio of the unconfined concrete core, where typically $\mu_o \approx 0.18$, $(f_o)_m$ = reference intercept stress in either the axial $(f_o)_c$ or radial $(f_o)_\theta$ strain direction, and $(k_o)_m$ = normalized reference intercept stress in either the axial $(k_o)_c$ or radial $(k_o)_\theta$ strain direction. In the above relationships the subscript m indicates the strain component under consideration, $(m = c)$ indicates an axial strain component, and $(m = \theta)$ indicates a radial (transverse) strain component. Also, the terms with the subscript *i* are evaluated at the limit radial strain where $(\varepsilon_{\theta p})_i = (\varepsilon_{\theta p})_{\lim}$ the terms with the subscript, *i*-1, are evaluated at $(\varepsilon_{\theta p})_{i-1} = \eta(\varepsilon_{\theta p})_{\lim}$ where $0.80 \le \eta \le 0.90$. By selecting a limiting radial strain, $(\varepsilon_{\theta p})_{\lim}$, in the FRP jacket such that $0.60\varepsilon_{\theta u} \le (\varepsilon_{\theta p})_{\lim} \le \varepsilon_{\theta u}$, and setting $(\varepsilon_{\theta p})_{\lim} = 12.5$ mm/m for GFRP confined concrete, and $(\varepsilon_{\theta p})_{\lim} = 8.5$ mm/m for CFRP confined concrete, sufficiently accurate plastic properties of the FRP-confined concrete could be obtained.

Assuming that both the FRP-confined and the unconfined concrete behave identically up to the critical dilation stress, $f_{cd} \approx 0.70 f_{co}$, which can be considered the axial stress at which the rate of volume dilation of the concrete core increases due to unrestrained crack propagation in the concrete core (Pantazopoulou 1995). As a result, the curvature parameter, n_m, of (14) can then be determined from the iterative solution of the following relationship:

$$\left(k_{Em}{}^{n_m}-1\right)^{\frac{1}{n_m}}-\left(\frac{E_m-E_{mp}}{E_{md}}\right)\frac{0.70}{\left(k_o\right)_m}=0;\;\; k_{Em}=\frac{E_m-E_{mp}}{E_{md}-E_{mp}};\;\; E_{md}=\frac{0.70 f_{co}}{\varepsilon_{md}}\approx\frac{E_m}{1.10} \quad (19)$$

where E_{md} = dilation secant modulus in either the axial $\left(E_{cd}\right)$ or radial $\left(E_{\theta d}\right)$ strain direction, and ε_{md} = axial $\left(\varepsilon_{cd}\right)$ or radial $\left(\varepsilon_{\theta d}\right)$ dilation strain at the axial dilation stress, $\left(f_{cd}\right)$.

In an FRP-confined concrete member, the compressive failure of the member occurs simultaneously with the failure of the FRP composite jacket, be it failure of the jacket due to rupture, delamination, lap failure or shear failure. Due to the interaction between the axial shortening and radial dilation which induces a biaxial state of stress and strain in the FRP-jacket, in addition to stress concentrations at the jacket-to-concrete interface that occur as the dilation of the concrete core progresses, failure of the FRP composite jacket can occur at an ultimate radial FRP jacket strain, $\varepsilon_{\theta u}$, that may be below the rupture strain of FRP composite tensile coupon tests. For circular concrete members confined by an FRP jacket having a high effective jacket stiffness, K_{je}, a non-iterative solution for the ultimate axial compressive strain, ε_{cu}, at the ultimate radial strain $\varepsilon_{\theta u}$ in the FRP jacket can be obtained by evaluating (13) at the ultimate jacket radial strain, where $\left(\varepsilon_{\theta p}\right)_i=\varepsilon_{\theta u}$.

The proposed stress-strain model was compared to experimental results and was found to accurately capture the bilinear compressive behavior of FRP confined concrete. The proposed model captures most of the experimental results, with some deviation at the onset of plastic behavior and at strains near failure.

CONCLUSIONS

A comprehensive model for representing the compressive behavior of concrete members confined by FRP composite jackets is presented. The proposed model is based on accepted concrete and FRP composite behavior, and fundamental principles of mechanics of materials, and it is applicable to both bonded and unbonded FRP-confined concrete. The distinguishing feature of the proposed model is a variable strain ductility ratio which was demonstrated to be a function of the stiffness of the confining FRP composite jacket and the extent of internal damage, rather than a constant as is typically assumed for steel confined concrete. The ultimate compressive strength and strain of the FRP confined concrete were found to be a function of the effective jacket stiffness, type of jacket construction (bonded or unbonded), and the ultimate strain in the FRP jacket. An expression for the ultimate axial compressive strain was derived herein based on equilibrium and a unique graphical analysis. Comparisons with experimental results indicate good agreement. The stress strain model as proposed herein can be easily implemented into a spreadsheet or other computer language program for evaluating the confinement effectiveness of FRP-confined concrete members.

AKNOWLEDGEMENTS

The research presented herein is part of continuing research at the Center for Composites in Construction at the University of Utah, sponsored by the Utah Department of Transportation (UDOT), and the Idaho National Engineering and Environmental Laboratories (INEEL). The authors wish to express their gratitude to Dr. Y. Xiao of USC for providing experimental data on carbon FRP confined concrete cylinders. The opinions expressed in this paper are those of the authors, and do not necessarily reflect the opinions of the sponsoring organizations.

REFERENCES

Darwin, D., and Pecknold, D. A. (1977). "Nonlinear biaxial stress-strain law for concrete." *J. Engrg. Mech. Div.*, *ASCE*, 103(2), 229-241.

Mander, J.B., Priestley, M.J.N., and Park, R. (1988). "Theoretical stress strain model for confined concrete." *J. Struct. Engrg., ASCE*, 114(8), 1804-1826.

Mirmiran, A., and Shahawy, M. (1996). "A new concrete–filled hollow FRP composite column." *Composites Part B: Engrg.,* 27B(3-4), 263-268, Elsevier Sci. Ltd, London, U.K.

Mirmiran, A. (1997). "Analytical and experimental investigation of reinforced concrete columns encased in fiberglass tubular jackets and use of fiber jacket for pile splicing." *Final Rep. Contract No. B-9135,* Florida Dept. of Transp., Tallahassee, Fla.

Mirmiran, A., and Shahawy, M. (1997a). "Behavior of concrete columns confined by fiber composites." *J. Structural Engrg.*, *ASCE*, 123(5), 583-590.

Mirmiran, A., and Shahawy, M. (1997b). "Dilation characteristics of confined concrete." *Mech. of Cohesive-Frictional Mat. Int. J.,* 2(3), 237-249.

Pantelides, C.P., Gergely, J., Reaveley, L.D., and Volnyy, V.A. (1999). "Retrofit of RC bridge pier with CFRP advanced composites." *J. Struct. Engrg.*, ASCE 125(10), 1094-1099.

Pantazopoulou, S.J. (1995). "Role of expansion on mechanical behavior of concrete." *J. Struct. Engrg.*, *ASCE*, 121(12), 1795-1805.

Pantazopoulou, S.J., and Mills, R.H. (1995). "Microstrucutural aspects of the mechanical response of plain concrete." *ACI Materials J.*, 92(6), 605-616.

Richard, R.M., and Abbott, B.J. (1975). "Versatile elastic-plastic stress-strain formula." *J. Engrg. Mech., ASCE,* 101(4), 511-515.

Richart, F.E., Brandtzaeg, A., Brown, R.L. (1928). "Study of the failure of concrete under combined compressive stresses." *Univ. of Illinois Engrg. Experiment Station, Bull.* No. 185, Urbana, Ill.

Saadatmanesh, H., Ehsani, M.R., and Li, M.W. (1994). "Strength and ductility of concrete columns externally reinforced with fiber composite straps." *ACI Struct. J.*, 91(4), 434-447.

Samaan, M., Mirmiran, A., and Shahawy, M. (1998). "Model of concrete confined by fiber composites." *J. Struct. Engrg.*, 124(9), 1025-1031.

Seible, F., Priestley, M.J.N., Hegemier, G.A., and Innamorato, D. (1997). "Seismic retrofit of RC columns with continuous carbon fiber jackets." *J. of Compos. for Constr.*, ASCE, 1(2), 52-62.

Spoelstra, M.R., and Monti, G. (1999). "FRP confined concrete model." *J. of Compos. for Constr.*, ASCE, 3(3), 143-150.

Stanton, J.F., Owen, L.M., and MacRae, G.A. (1998). "Stress-strain properties of confined concrete." *Proc. Sixth Intern. Conf. on Earthq. Engrg.*, *EERI*, Oakland, Ca.

Wu, H., and Xiao, Y. (2000). "Compressive stress-strain behavior of concrete confined by carbon fiber jackets." *Proc. Sixth ASCCS Conf.*, Los Angeles, Ca., 919-926.

Xiao, Y., and Ma, R. (1997). “Seismic retrofit of RC circular columns using prefabricated composite jacketing.” *J. Struct. Engrg., ASCE*, 123(10), 1357-1364.

Xiao, Y., and Wu, H. (2000). “Compressive behavior of concrete confined by carbon fiber composite jackets.” *J. of Materials in Civil Engineering*, 12(2), 139-146.

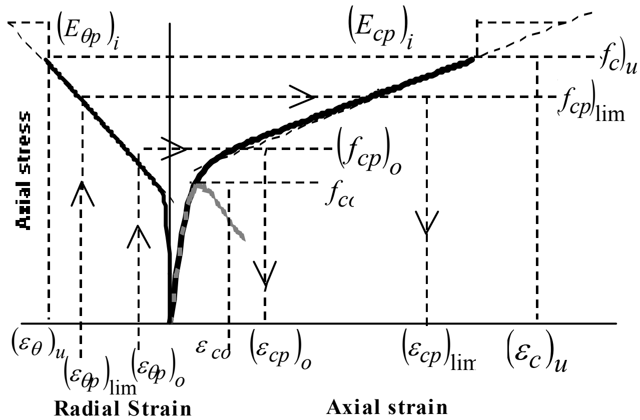

Fig. 1. Typical stress strain behavior of FRP confined concrete exhibiting strain hardening

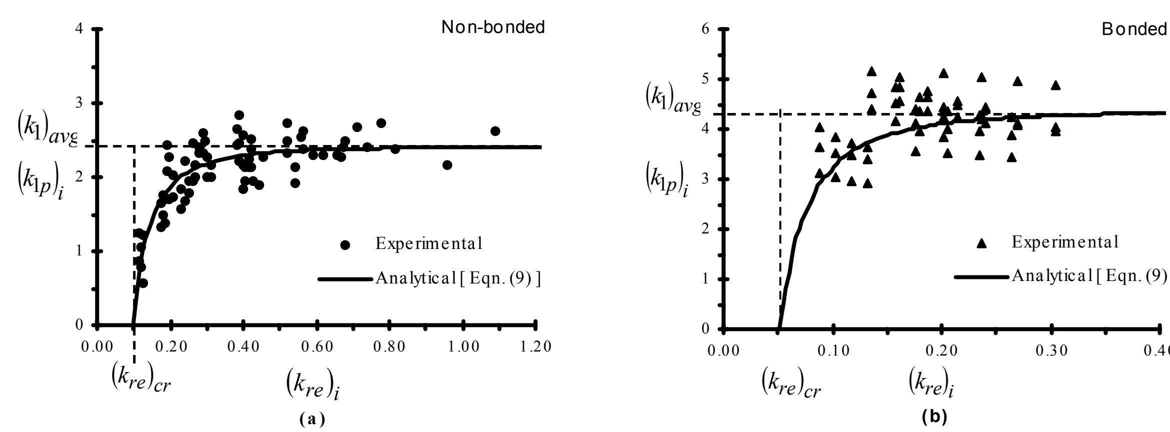

Fig. 2 Experimental plastic confinement coefficient versus effective confinement ratio for: (a) non-bonded and (b) bonded FRP confined concrete

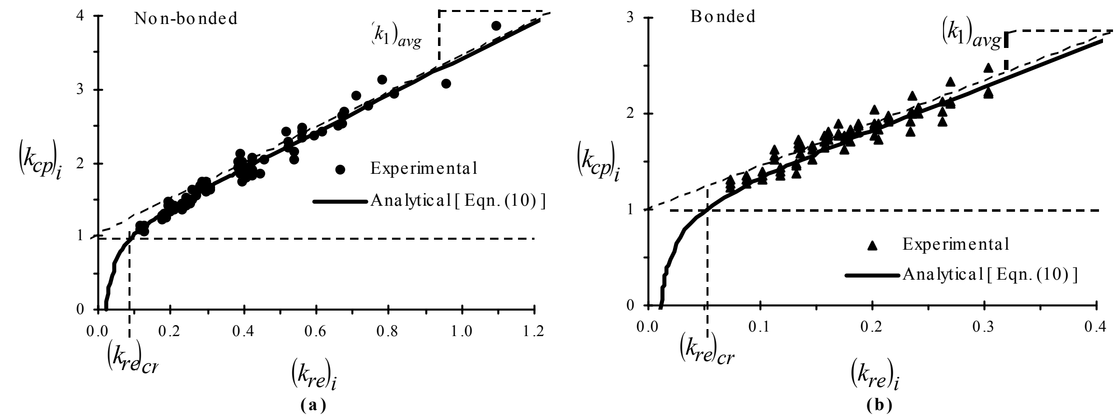

Fig. 3 Experimental plastic confinement effectiveness versus effective confinement ratio: (a) non-bonded and (b) bonded FRP confined concrete

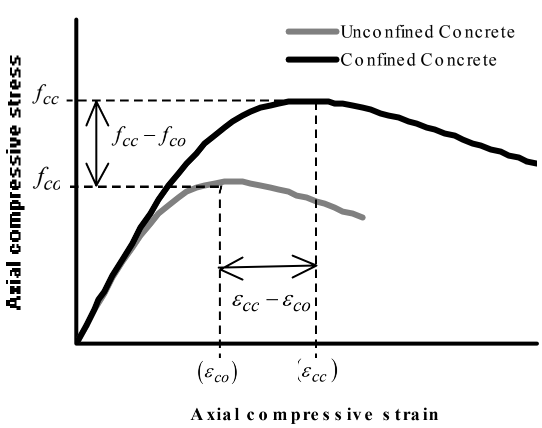

Fig. 4 Strain ductility ratio for steel confined concrete

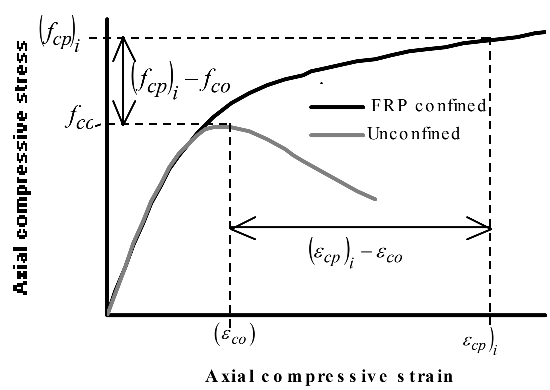

Fig. 5 Variable plastic strain ductility ratio in FRP confined concrete

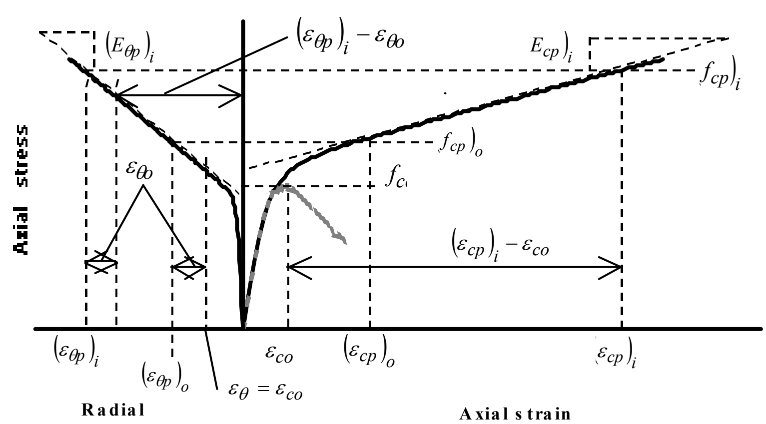

Fig. 6 Determination of variable axial plastic compressive strain ratio

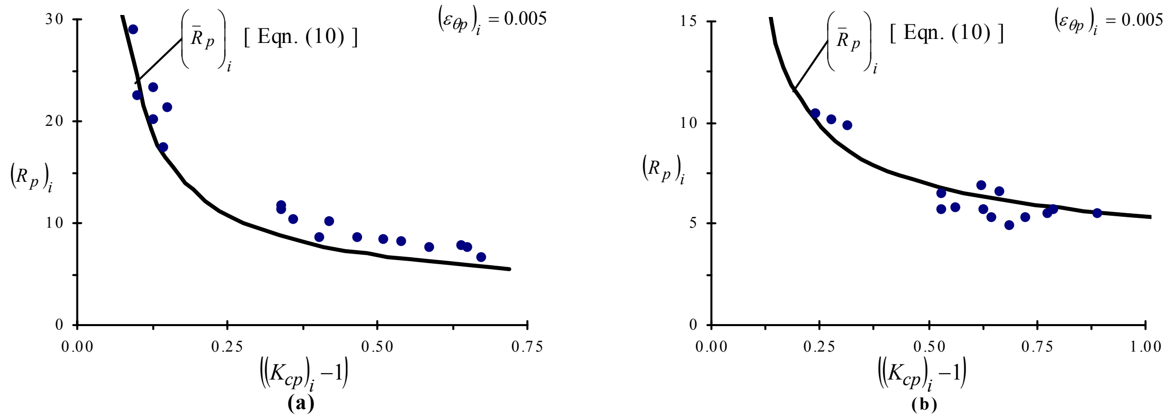

Fig. 7 Experimental and analytical variable strain ductility ratio versus confinement stress ratio: (a) non-bonded and (b) bonded FRP-confined concrete

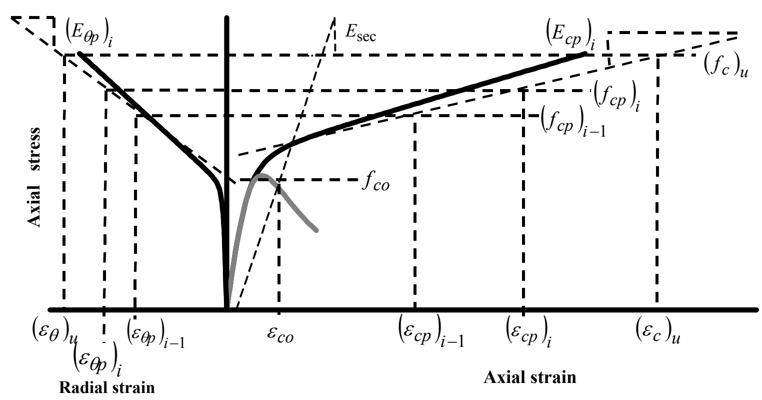

Fig. 8 Determination of plastic stress-strain properties of FRP confined concrete

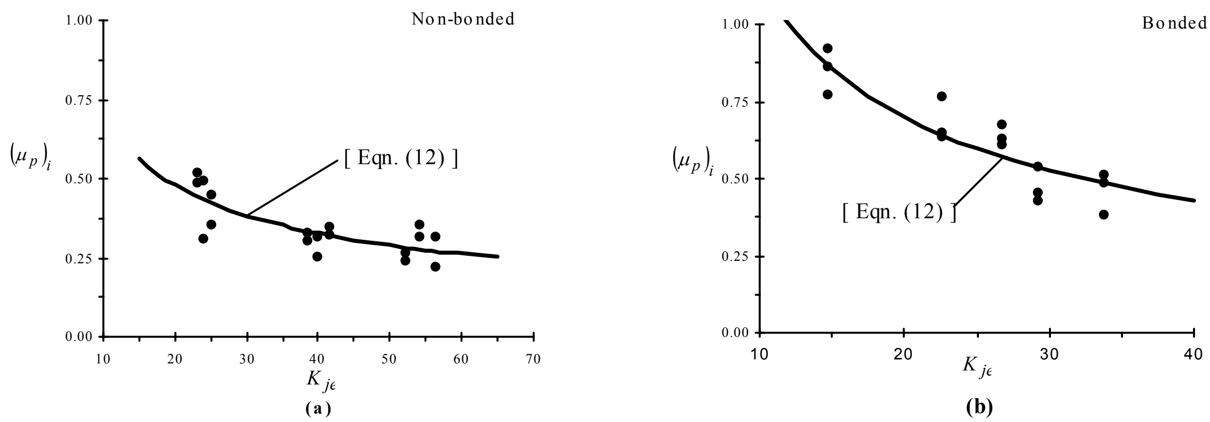

Fig. 9 Plastic dilation rate versus effective jacket confining stiffness of FRP confined concrete: (a) non-bonded and (b) bonded

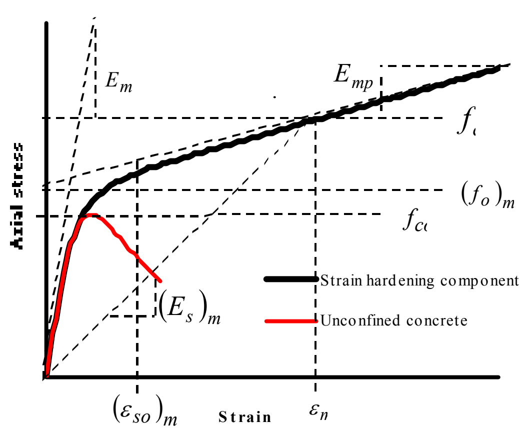

Fig. 10 Determination of bilinear stress-strain parameters of FRP confined concrete